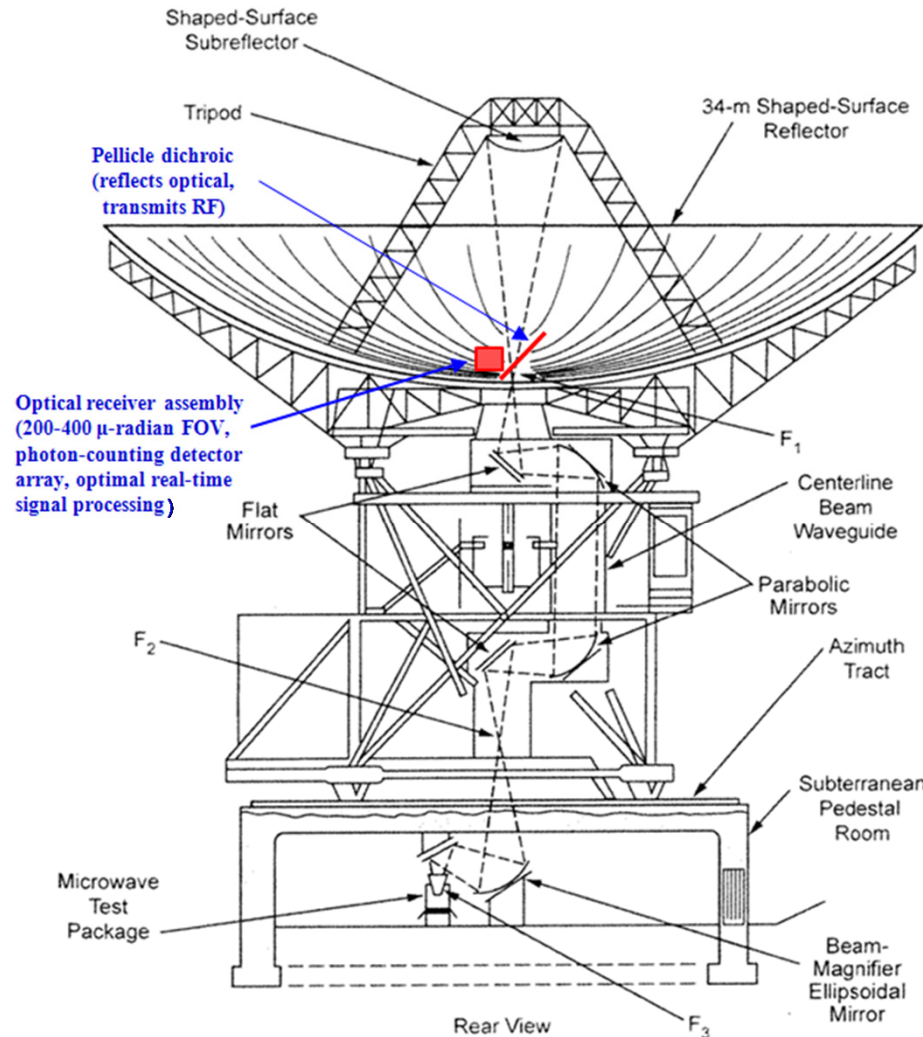
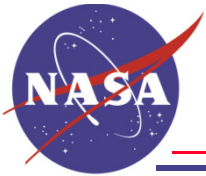


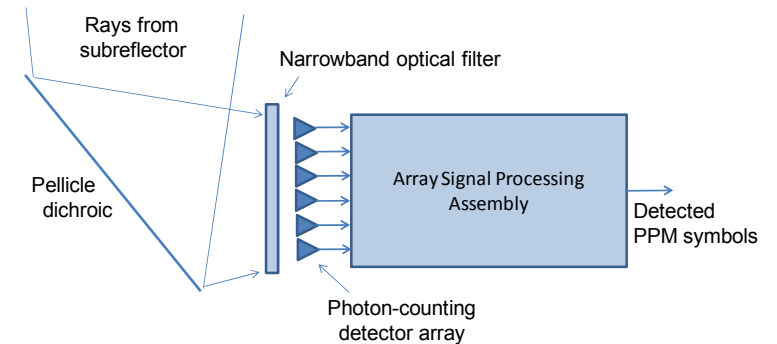
Large Aperture “Photon Bucket” Optical Receiver Performance in High Background Environments

V. Vilnrotter, D. Hoppe

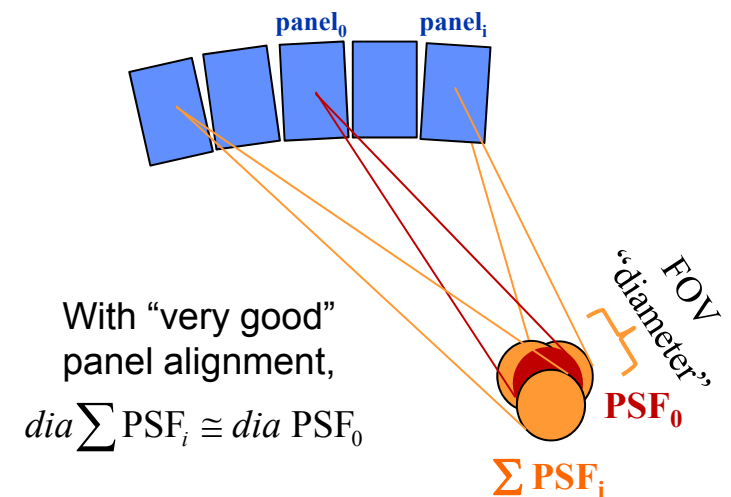
Jet Propulsion Laboratory
California Institute of Technology

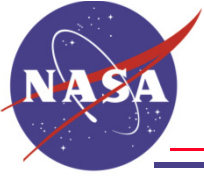


Optical communications receiver assembly placed at F1: RF/Optical dichroic, optical filter, detector array, high-speed signal-processing equipment.



Functional block diagram of Optical Receiver Assembly, placed on the main reflector at F1, near the entrance to the RF beam waveguide in a DSN 34-meter antenna.





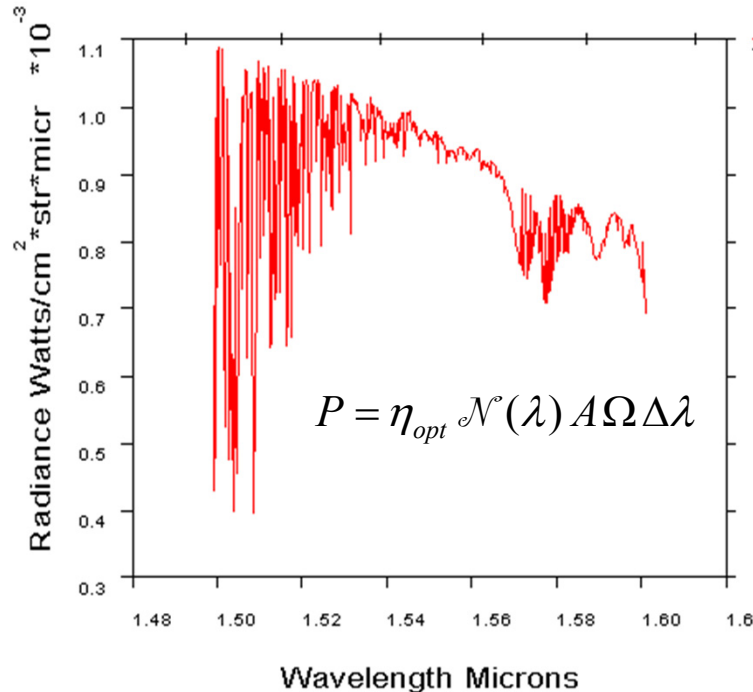
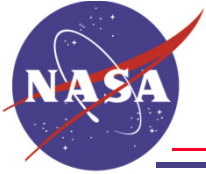
DSN polished panel, initial daytime visual tests



DSN polished panel reflectivity, surface accuracy test



DSN polished panel ray concentration



Example of sky radiance for a desert model, at “sun-earth-probe” (SEP) angle of 10 degrees.

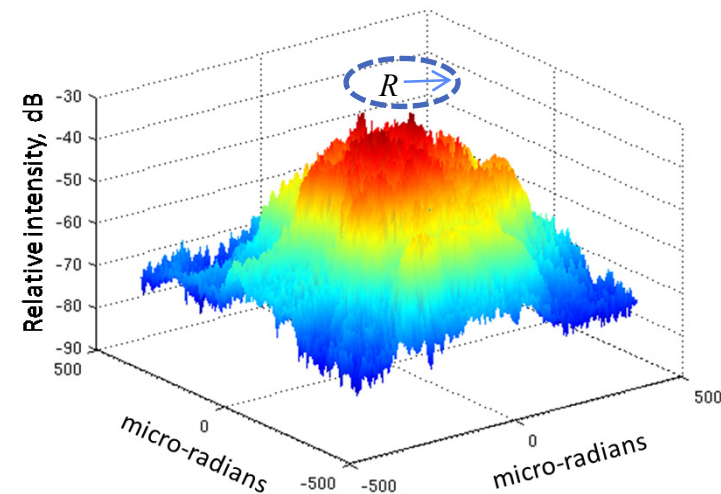
$$\Omega = \pi R^2 / f_{eff}^2$$

$$n_b = \eta_{opt} \eta_d \pi R^2 \mathcal{N}(\lambda) A \Delta\lambda / h \nu f_{eff}^2$$

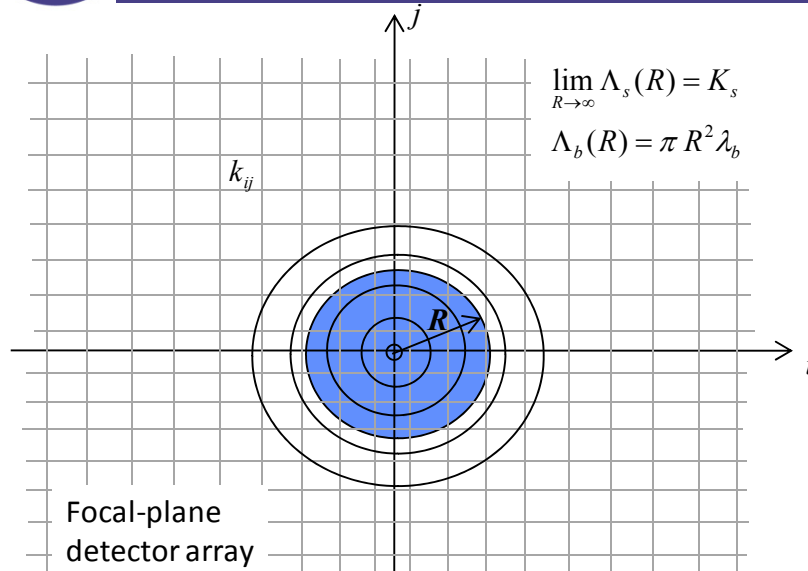
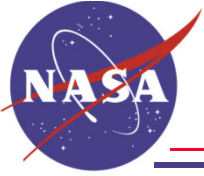
$$K_b = \eta_{opt} \eta_d \mathcal{N}(\lambda) A \Omega \Delta\lambda \tau / h \nu \equiv I_b A$$

Average background count K_b depends on background intensity in photo-counts/meter², and collecting area A in meter²

- $\mathcal{N}(\lambda)$ - Spectral radiance function
- A - Receiver collecting area
- Ω - Receiver FOV, steradians
- λ - Optical signal wavelength
- $\Delta\lambda$ - Narrowband filter bandwidth
- η_{opt} - Optical system throughput
- η_d - Detection efficiency



Example of PSF generated by a realistically modeled panel surface error distribution, showing high concentration of signal energy in the inner +/- 125 micro-radians from center. Horizontal axes in μ rad, vertical axis in dB (intensity, arbitrary units)



Detector-plane model of photon-counting Array and PSF with small pointing offsets.

Poisson calculation:

$$P_M^l(C) \geq \sum_{k=1}^{\infty} \frac{(\Lambda_s(R) + \Lambda_b(R))^k}{k!} \exp[-(\Lambda_s(R) + \Lambda_b(R))] \times \left\{ \sum_{j=0}^{k-1} \frac{(\Lambda_b(R))^j}{j!} \exp[-(\Lambda_b(R))] \right\}^{M-1}$$

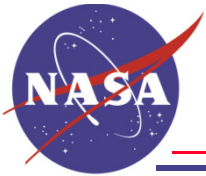
$$P_M^u(E) \equiv 1 - P_M^l(C) \geq P_M(E) \cong P_M(E)$$

Gaussian approximation:
$$P_M(C) \cong \int_{-\infty}^{\infty} dy Gsn[\Lambda_s(R) + \Lambda_b(R), y] \left[\int_{-\infty}^y dx Gsn[\Lambda_b(R), x] \right]^{M-1}$$

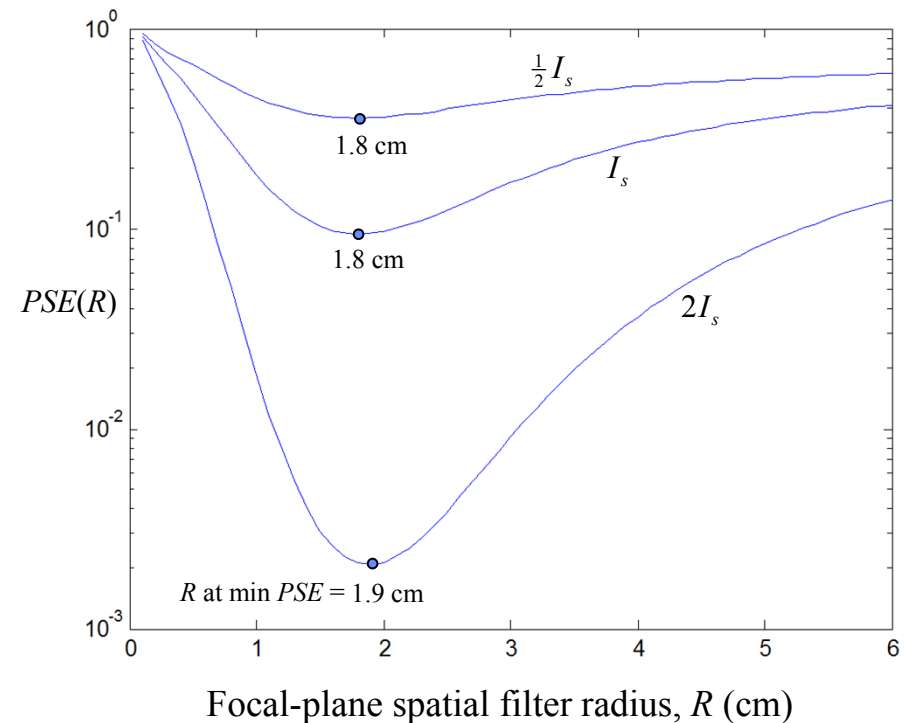
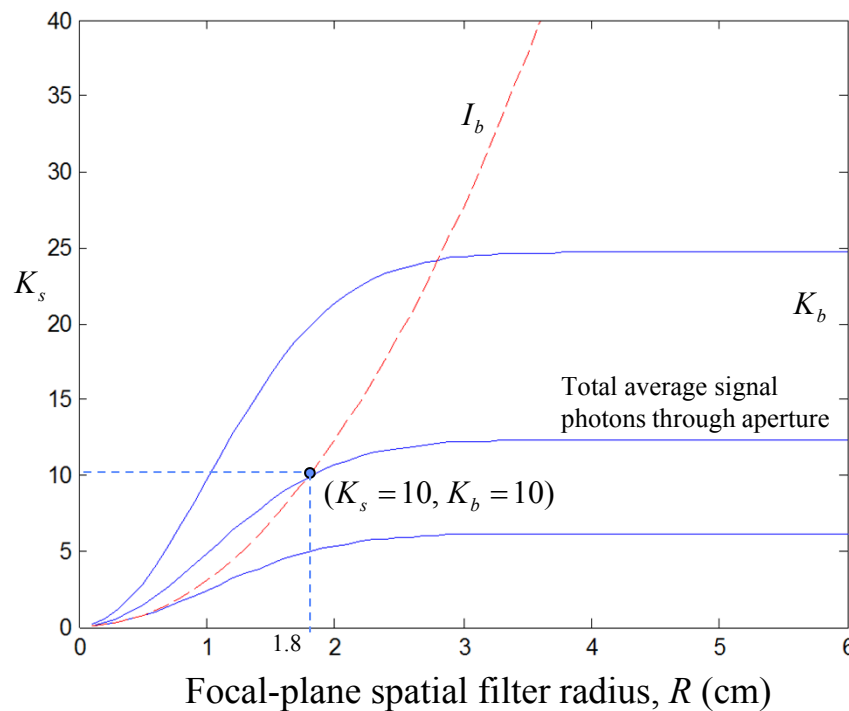
- Laser transmitter appears as a point source, therefore ...
- Average signal count can be expressed as: $K_s = I_s A$
- With fixed field-of-view Ω , the average background count can be expressed as: $K_b = I_b A$

$$\Delta K_s = I_s \Delta A$$

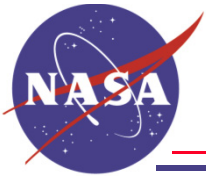
$$\Delta K_b = I_b \Delta A = (I_b / I_s) \Delta K_s$$



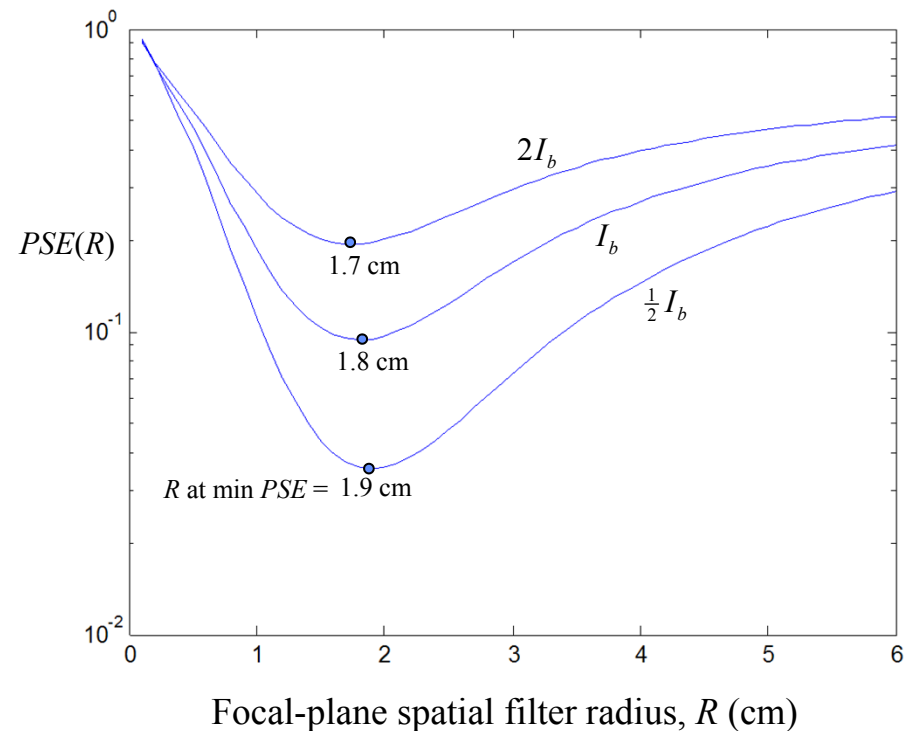
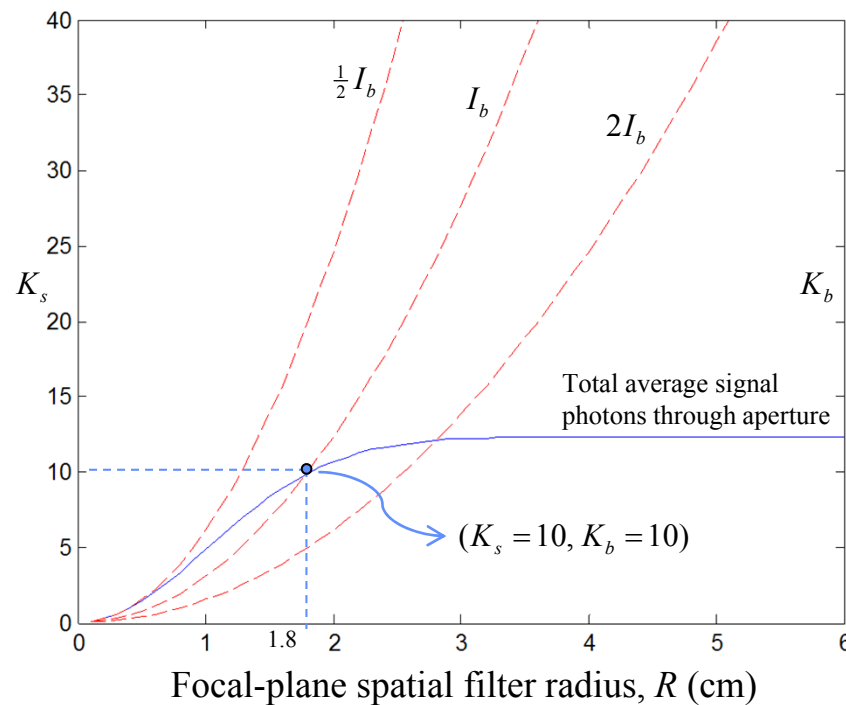
Focal-plane optimization with constant background intensity



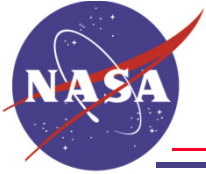
2D Gaussian PSF model, standard deviation $\sigma_{PSF} = 1$ cm



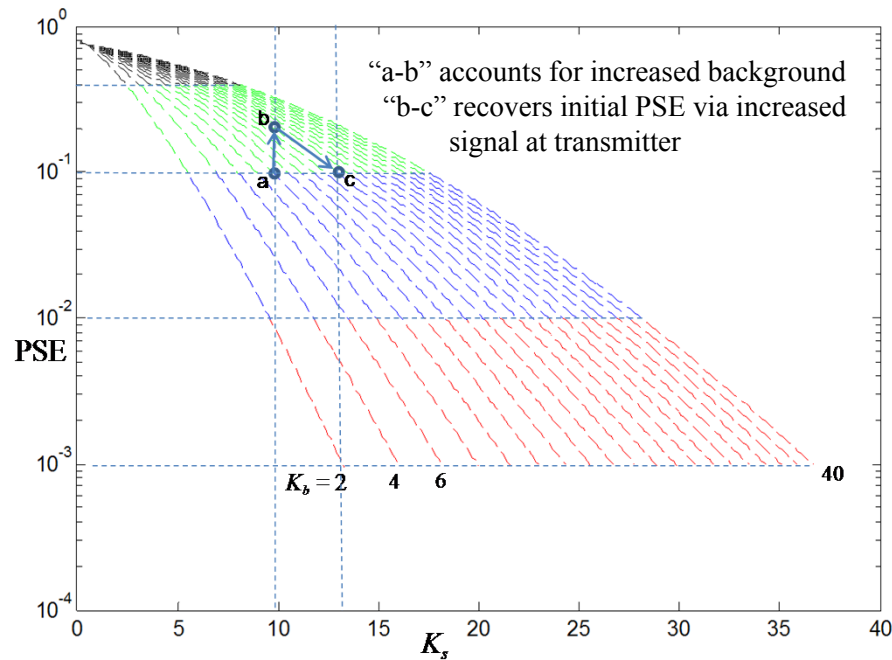
Focal-plane optimization with constant signal intensity



2D Gaussian PSF model, standard deviation $\sigma_{PSF} = 1$ cm

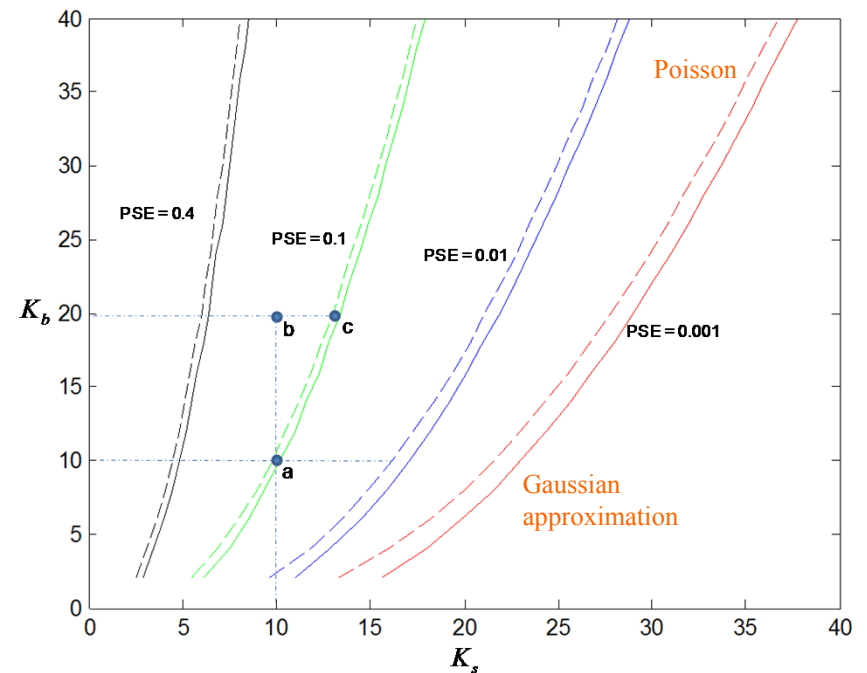


Poisson computation of PSE vs K_s

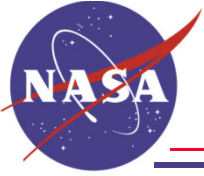


Probability of symbol error, PSE, for $M = 4$ PPM signaling as a function of K_s , for a range of background energies, K_b .

Constant PSE contours, (K_s, K_b) plane



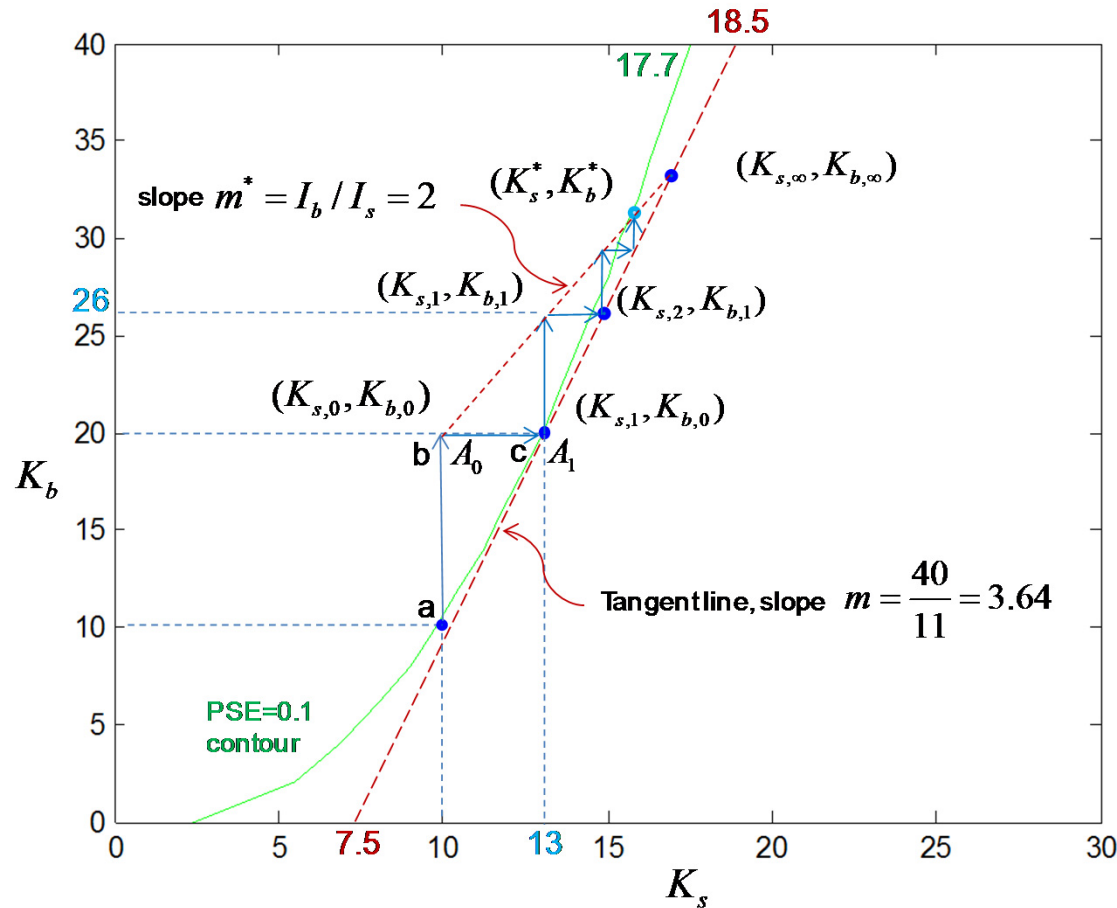
Contours of constant symbol-error probability, PSE, over the (K_s, K_b) plane. Dashed curves were computed using Poisson probabilities, solid curves computed via the faster Gaussian approximation.



IEEE AEROSPACE CONFERENCE, MARCH 2011

Tangent-Line Approximation and Exact Solution

Jet Propulsion Laboratory
California Institute of Technology



Compensation for excess background energy by increasing signal energy via aperture expansion, with the goal of maintaining constant symbol-error probability of PSE = 0.1.

$$K_{s,1} = K_{s,0} + \Delta K_{s,1} = I_s (A + \Delta A_1)$$

$$K_{b,1} = K_{b,0} + \Delta K_{b,1} = I_b (A + \Delta A_1)$$

$$= \frac{I_b}{I_s} (K_{s,0} + \Delta K_{s,1})$$

$$K_{s,2} = K_{s,0} + \Delta K_{s,1} + \frac{I_b}{I_s m} \Delta K_{s,1}$$

$$K_{s,3} = K_{s,0} + \Delta K_{s,1} + \frac{I_b}{I_s m} \Delta K_{s,1} + \left(\frac{I_b}{I_s m} \right)^2 \Delta K_{s,1}$$

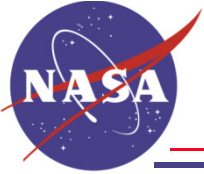
$$K_{s,\infty} = K_{s,0} + \Delta K_{s,1} \sum_{k=0}^{\infty} (I_b / I_s m)^k$$

$$= K_{s,0} + \Delta K_{s,1} (1 - \frac{I_b}{I_s m})^{-1}$$

$$= K_{s,0} + \Delta K_{s,1} \alpha / (\alpha - 1); \quad \alpha = I_s m / I_b$$

$$\text{Similarly for } K_b : K_{b,\infty} = (I_b / I_s) K_{s,\infty}$$

$$\text{for } \alpha > 1 \text{ since } \lim_{\alpha \rightarrow 1} \alpha / (\alpha - 1) = \infty$$



Example: $K_{b,0} = 20, \quad K_{s,0} = 10, \quad \Delta K_{s,1} \cong 3, \quad \Delta K_{b,1} \cong 6,$

$$m = 40/11 = 3.64 \qquad \alpha / (\alpha - 1) = 2.22$$

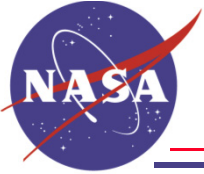
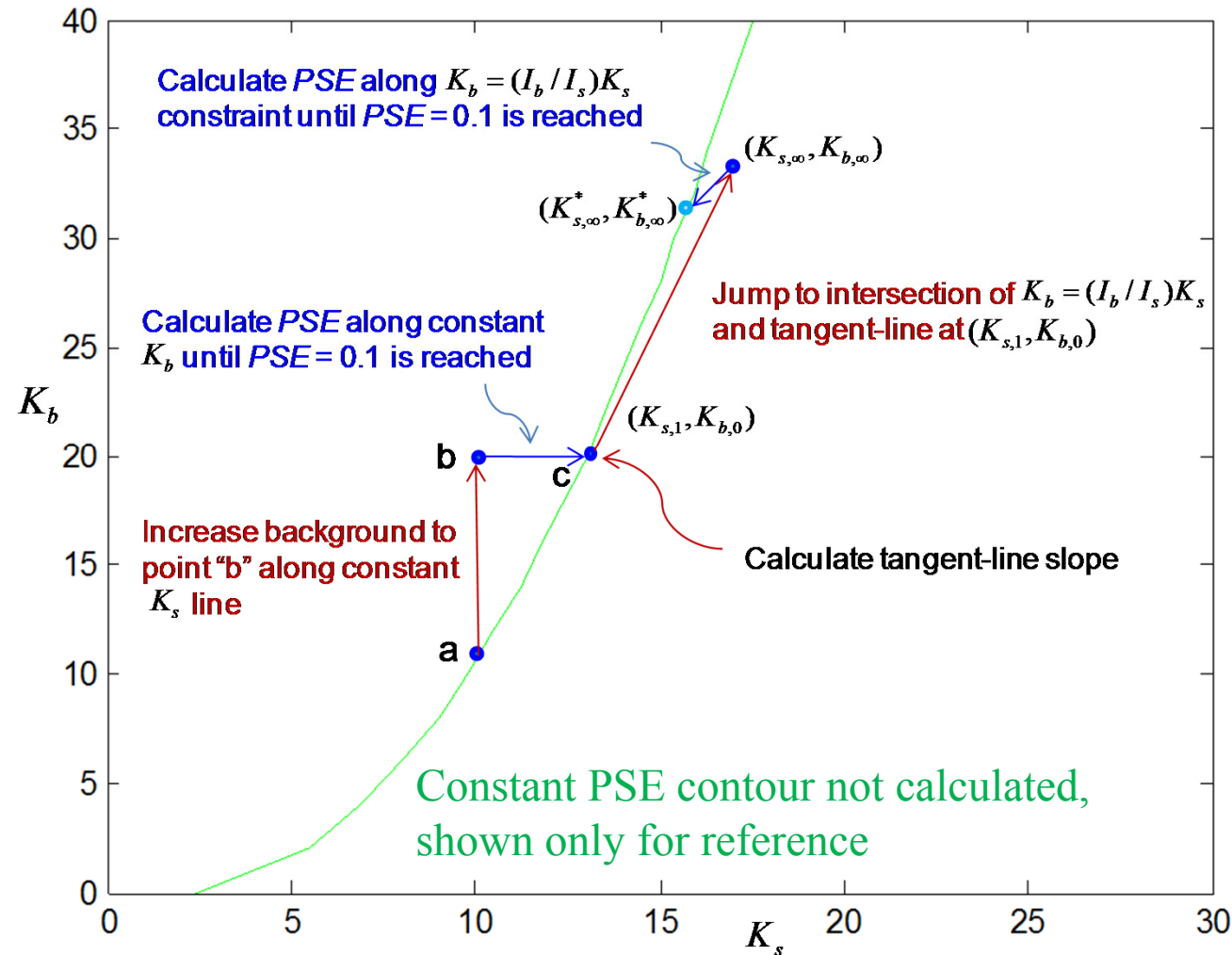
$$K_{s,\infty} = 10 + 6.67 = 16.67 \qquad K_{b,\infty} = 2K_{s,\infty} = 33.3$$

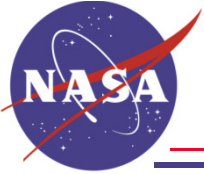
$$(K_{s,i}, K_{b,i}), \quad i = 0, 1, 2, \dots \qquad m^* = I_b / I_s$$

$$(K_s^* = 15.5, K_b^* = 31.5)$$

$$\Delta A \cong 55\% \quad \Delta D \cong 24\%$$

Therefore, only 55% increase in receiver collecting area (or 24% increase in receiver diameter) is required to compensate for 100% increase in background energy.

Proposed “simpler” algorithm for calculating final (K_s, K_b) values



Other potential “simpler” algorithms

1. Gaussian approximation:

- Compute *PSE* contour using the Gaussian approximation
- Determine intersection of $K_b = (I_b / I_s) K_s$ line with Gaussian contour
- Calculate *PSE* along $K_b = (I_b / I_s) K_s$ constraint

2. Constrained trajectory solution:

- Starting at (0,0) calculate *PSE* along the $K_b = (I_b / I_s) K_s$ trajectory using Poisson model until desired *PSE* is reached

Evaluation and Comparison of Reduced Complexity Algorithms
remains the subject of future work